applied sciences

MDPI

Article

Use of Treated Non-Ferrous Metallurgical Slags as Supplementary Cementitious Materials in Cementitious Mixtures

Asghar Gholizadeh Vayghan [1,*], Liesbeth Horckmans [1], Ruben Snellings [1], Arne Peys [1], Priscilla Teck [1], Jürgen Maier [2], Bernd Friedrich [2] and Katarzyna Klejnowska [3]

1 Sustainable Materials Management, VITO, 2400 Mol, Belgium; liesbeth.horckmans@vito.be (L.H.); ruben.snellings@vito.be (R.S.); arne.peys@vito.be (A.P.); priscilla.teck@vito.be (P.T.)
2 IME Process Metallurgy and Metal Recycling, RWTH Aachen University, 52072 Aachen, Germany; JMaier@metallurgie.rwth-aachen.de (J.M.); bfriedrich@metallurgie.rwth-aachen.de (B.F.)
3 Łukasiewicz Research Network—Institute of Non-Ferrous Metals, Ul. Sowińskiego 5, 44-100 Gliwice, Poland; katarzyna.klejnowska@imn.gliwice.pl
* Correspondence: asghar.gholizadehvayghan@vito.be; Tel.: +32-14-33-57-57

Abstract: This research investigated the possibility of using metallurgical slags from the copper and lead industries as partial replacement for cement. The studied slags were fayalitic, having a mainly ferro-silicate composition with minor contents of Al_2O_3 and CaO. The slags were treated at 1200–1300 °C (to reduce the heavy metal content) and then granulated in water to promote the formation of reactive phases. A full hydration study was carried out to assess the kinetics of reactions, the phases formed during hydration, the reactivity of the slags and their strength activity as supplementary cementitious material (SCM). The batch-leaching behaviour of cementitious mixtures incorporating treated slags was also investigated. The results showed that all three slags have satisfactory leaching behaviour and similar performance in terms of reactivity and contribution to the strength development. All slags were found to have mediocre reactivity and contribution to strength, especially at early ages. Nonetheless, they passed the minimum mechanical performance requirements and were found to qualify for use in cement.

Keywords: sustainability; non-ferrous metallurgical slag; supplementary cementitious materials; hydration study; batch leaching

check for updates

Citation: Gholizadeh Vayghan, A.; Horckmans, L.; Snellings, R.; Peys, A.; Teck, P.; Maier, J.; Friedrich, B.; Klejnowska, K. Use of Treated Non-Ferrous Metallurgical Slags as Supplementary Cementitious Materials in Cementitious Mixtures. *Appl. Sci.* **2021**, *11*, 4028. https://doi.org/10.3390/app11094028

Academic Editor: Theodore E. Matikas

Received: 31 March 2021
Accepted: 25 April 2021
Published: 28 April 2021

Publisher's Note: MDPI stays neutral with regard to jurisdictional claims in published maps and institutional affiliations.

Copyright: © 2021 by the authors. Licensee MDPI, Basel, Switzerland. This article is an open access article distributed under the terms and conditions of the Creative Commons Attribution (CC BY) license (https://creativecommons.org/licenses/by/4.0/).

1. Introduction

Portland cement continues to have the highest share of CO_2 emission among all construction materials [1] and is responsible for 5–8% of the total anthropogenic CO_2 emission across the planet [2]. Researchers in the past few decades have attempted to reduce the use of clinker in cement-based materials by partially or fully replacing the clinker with supplementary cementitious materials (SCMs) or alternative binders. Some notable SCMs with established environmental and technical benefits when used with Portland cement are silica fume, coal fly ash, and granulated blast furnace slag from iron production. From the environmental point of view, their use in combination with Portland cement not only eliminates the need for their disposal (which is favourable due to the lack of landfill spaces) but also reduces the environmental impact of cement-based materials (by reducing their CO_2 footprint and embodied energy). In addition, the incorporation of such SCMs in concrete entails numerous technical benefits such as higher durability against corrosion, sulphate attack and alkali–silica reaction and often improved long-term mechanical properties [3–6].

The slags generated during pyrometallurgical processes in the lead or copper production industry are investigated and used in cement and concrete to a much lower extent [7] compared to the typical SCMs mentioned earlier. While smaller amounts of such slags

are produced compared to iron slag (5.5 and 68.7 million tons for lead and copper slags, respectively [7,8], compared to 320–384 million tons for iron slag [9] on a global basis), they often incorporate considerably higher amounts of heavy metals and corrosive anions [7,10], which makes their disposal more critical and costly. Their use in concrete also comes with the risk of disturbing the cement hydration reactions (due to the presence of sulphates, other anions and heavy metals) and leaching of contaminants to the environment in the long term. As such, a separate pyrometallurgical treatment can be applied to such slags to recover the valuable heavy metals such as metallic lead and zinc, reduce the toxic heavy metals such as arsenic and antimony and remove the anions. The application of this step is intuitively crucial for converting such slags from wastes into secondary resources with the potential for being used in the cement and concrete industry as SCMs or precursors of alkali-activated materials [7,8,11–13]. The thermal treatment usually involves melting the slags intermixed with coke at up to 1200–1300 °C, followed by dwelling at such temperature for a length of time to fume off volatile elements and reduce others to a metallic state that can be tapped. To promote the reactivity of the slags, they are rapidly granulated in water to avoid crystallisation and the formation of stable phases [14,15]. Some additives such as silica and limestone may be added to the slag prior to the thermal treatment as flux to reduce the ultimate temperature, optimise the melt viscosity and/or increase the reactivity as SCMs or in alkaline media in general [3,7,16–18].

Ariño and Mobasher [3] studied the effects of using a source of copper slag on the mechanical properties of concrete and found out that replacement of 10% of Portland cement with rapidly cooled granulated slag resulted in a slight increase in the compressive strength. Edwin et al. [19] used two sources of slowly cooled and rapidly cooled copper slag (milled for two different milling times) in combination with Portland cement up to 20% replacement. They concluded that low replacement levels can enhance the hydration reactions, while higher levels of replacement can cause some retardation. Rapid cooling was found to slightly enhance the strength activity of the slags, and the fineness was found to have a mild influence on the strength activity index (SAI) of the slags. Hallet et al. [20] studied the effect of fineness of a non-ferrous metallurgical slag (NFMS) on the reactivity of blended cements [20]. They also reported a slightly higher long-term strength for finer slag despite the retarding effect of the fineness on early-age hydration. The R3 heat release results of the NFM slags studied by Hallet et al. [20] and Sivakumar et al. [21] suggest that—when rapidly cooled—these slags can exhibit a higher reactivity than coal fly ash.

Few studies can be found in the literature systematically investigating the effects of copper and especially lead slag composition and mineralogy on the hydration reactions and microstructural development of Portland cement systems. The reactive phases contributing to pozzolanic reactions are not well characterised, and the effects of treatment conditions and the rate of cooling on the crystalline structure of the slags and its influence on their chemical reactivity are barely explored. The leaching behaviour of concrete incorporating such slags is also not well known.

This research is a systematic attempt towards studying the properties of copper and lead slags and their technical and environmental performances in cementitious mixtures. A full hydration study was carried out on two sources of slag generated in copper and lead production industries, along with a synthetically produced ferro-silicate slag. The slags were characterised, and their composition, mineralogy, chemical reactivity, pozzolanic performance, influence on cement hydration and microstructural development were comprehensively investigated. The performance and reactivity of the slags were compared with other typical SCMs and standard requirements. The environmental behaviour of the hardened mixtures incorporating such slags was also quantified as per the batch-leaching test and compared with the existing standard limitations.

2. Materials and Methods

2.1. Materials

A sample of slag generated in the smelting process of copper (S1) and one generated from the smelting process of primary/secondary lead concentrates (S2) along with a synthetic ferro-silicate slag (S3) are studied in this research. S3 is included in this research to account for slags with extreme chemical compositions (low silica and alumina and high iron oxide contents) in order to investigate how such compositions will perform in cementitious mixtures. The alkali content in this slag is also considerably lower than in S1 and S2. Due to the high heavy metal and sulphates content of the slags, they are first pyrometallurgically treated, as described here, in order to recover valuable metals and remove toxic heavy metals and sulphates. S1 was treated in a top-submerged lance furnace by combustion at 1200–1300 °C (20% coke addition) for 4 h, followed by rapid cooling in water. The rationale behind rapid cooling, which is applied to all three slag sources, is to avoid crystallisation and promote chemical reactivity [14,15,22,23]. The treated slag is referred to as TS1 (short for treated S1). S2 was treated in an electric-arc furnace at a similar ultimate temperature (with 5% coke added) for 2 h and then rapidly cooled in water (treated slag labelled TS2). The synthetic slag (S3) was first produced by mixing metallurgical materials such as Waelz kiln slag, Waelz kiln oxide, PnSnSb oxide dross, PbAs converter dust and silica sand. It was then combusted in a top-submerged lance furnace (15% coke addition) at a similar temperature for 3.5 h, followed by rapid cooling (TS3). Table 1 shows the oxide composition of the slags, along with the metal contents before and after treatment. It is observed that all slags originally contained considerable amounts of zinc and lead, which are successfully reduced and recovered by the applied treatments (compare the zinc oxide and lead contents of each slag in the raw and treated states). Heavy metals are also reduced as a result of treatment. However, the high pH of the cement pore solution can promote the leaching of elements such as lead [24–26], which needs to be measured and evaluated via batch-leaching experiments, as laid out later in Section 2.2.

Table 1. The oxide and elemental composition of raw and treated slags.

	Oxide/Metal	Slag Source					
		S1 (Raw)	S2 (Raw)	S3 (Synthetic)	TS1 (Treated)	TS2 (Treated)	TS3 (Treated)
Oxide content (%)	FeO	13.5	21.9	35.3	16.9	21.6	31.0
	SiO_2	18.5	17.3	20.6	50.6	39.0	21.3
	CaO	5.64	7.28	9.66	9.45	15.8	9.93
	Al_2O_3	4.25	2.15	2.68	11.0	11.8	5.67
	Na_2O	7.04	2.72	0.67	9.32	5.76	3.06
	K_2O	2.10	0.55	0.51	2.54	0.42	0.73
	MgO	4.21	0.28	2.82	5.84	7.96	0.65
	ZnO	7.19	10.7	12.9	0.18	0.03	1.45
	CuO	0.72	0.05	0.23	0.18	0.08	0.01
	SO_3	17.3	<0.05	0.77	0.49	0.29	0.32
Metal content (%)	Pb	3.48	3.86	4.45	0.001	0.001	0.075
	As	0.409	0.505	0.14	<0.001	<0.001	0.006
	Sn	0.179	0.304	0.93	0.001	0.004	0.214
	Sb	0.037	0.628	0.54	<0.001	0.001	0.027
	Co	0.008	0.011	NA	<0.001	<0.001	0.005

From the chemistry standpoint, the slags are primarily composed of ferro-silicates, with the lowest iron oxide content and the highest silica content belonging to TS1 among the three slags (16.9% and 50.6%, respectively). TS3, in contrast, contains the highest iron oxide and the lowest silica content (31.0% and 21.3%, respectively), and TS2 contains intermediate amounts of each oxide (21.6% and 39.0%, respectively) in comparison with TS1 and TS3. TS2 also contains the highest calcium oxide and alumina contents in comparison

with TS1 (also high in alumina) and TS3 (particularly low alumina content). Nonetheless, all three slags are lean in calcium oxide, which is probably not favourable in terms of reactivity [16,17,27]. It is evident that there are substantial differences in the composition of such slags with typical blast furnace slags (BFS). According to EN 15167-1, the composition of BFS shall be such that two-thirds of its mass is composed of SiO_2, CaO and MgO and that (CaO + MgO)/SiO_2 exceeds 1.0. Such criteria are not met in any of the three slags investigated in this research. Moreover, all slags contain exceeding amounts of alkalis (equivalent alkali contents are, respectively, 11.0%, 6.0% and 3.5% for TS1, TS2 and TS3; EN 15167-1 limit on $Na_2O_{eq.}$: 1.2%), which are added as flux to decrease the liquidus temperature of the slags and thus decrease the potential operating temperature of the metallurgical process. This is especially the case in lead metallurgy, where the melting temperature of the metal phase is low. This could further increase the pH of the cement pore solution, which can, in turn, exacerbate the leaching of lead [24–26]. However, if the alkalis are in the glassy phases of the slags, they would then not necessarily dissolve into the pore solution and contribute to its alkalinity [28].

The phase composition of the slags was analysed via X-ray diffractometry. Figure 1 shows the X-ray diffraction patterns of TS1, TS2 and TS3. The XRD data were collected using an Empyrean diffractometer (Panalytical) equipped with a CoKα tube. The tube operating conditions were 40 kV and 45 mA. Diffraction scans were recorded from 5 to 110 °2θ, with a step size 0.013 °2θ and a measurement time per step of 50 s.

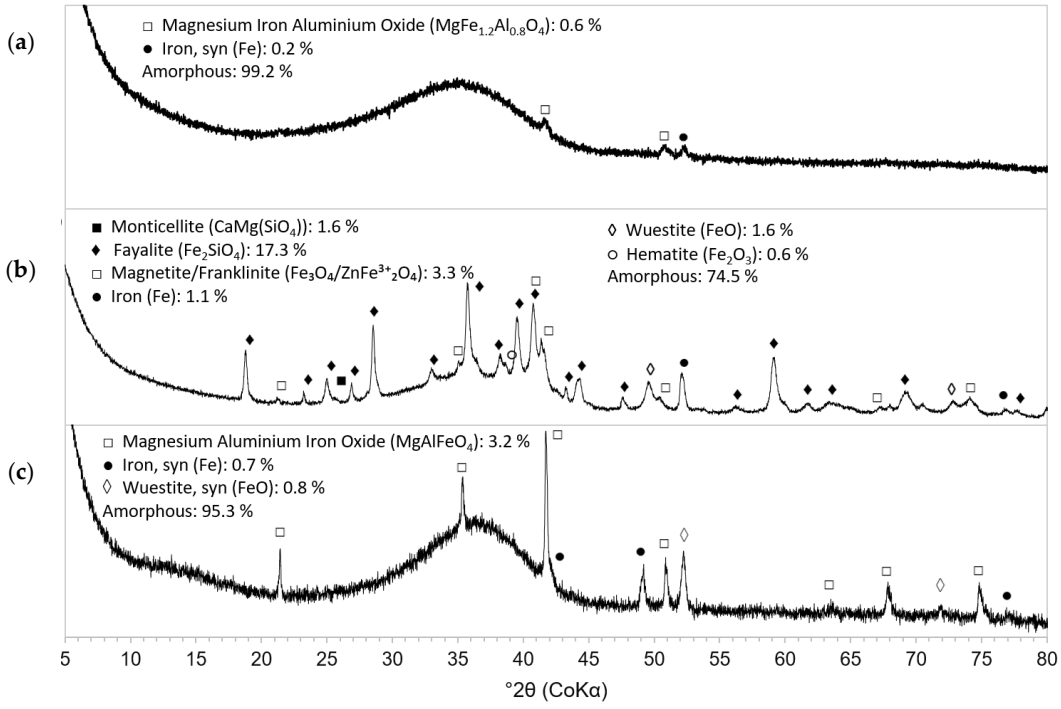

Figure 1. XRD patterns and phase quantification results of the treated slags: (**a**) TS1, (**b**) TS2 and (**c**) TS3.

Rietveld analysis was performed using HighScore Plus software (version 4.6a), and the external standard approach was used to determine the amorphous phase content (rutile; Kronos 2300 TiO_2 external standard calibrated against NIST SRM 676a α-Al_2O_3). The mass attenuation coefficients needed for the absorption correction were calculated using the chemical composition results listed in Table 1. The crystalline phases were identified for each slag and listed with their respective mass fractions and the mass fraction of the XRD amorphous phase(s) on each diffractogram (see Figure 1). TS1 is an amorphous material (99.2% amorphous content) with trace amounts of magnesium iron aluminium oxide and metallic iron. The primary crystalline phase in TS2 (which is the most crystalline slag among the three studied slags) is fayalite comprising 17.3% of the total mass. Minor

amounts of magnetite/franklinite, wuestite, monticellite and metallic iron are also detected in TS2, while 74.5% of the slag is composed of amorphous phases. TS3 contains a higher amorphous content (95.3%; comparable to that of TS1) with minor amounts of crystalline phases such as magnesium aluminium iron oxide, wuestite and metallic iron.

The treated slags were milled using a planetary ball mill at 400 rpm for 10 min. The particle size distributions of the slags were measured using a Horiba laser diffraction particle size analyser in isopropyl alcohol. Representative samples were dispersed in isopropyl alcohol by stirring and ultrasound prior to testing (the refractive index of the slag is assumed to be 2.3–0.05 × i, which is suitable for high-ferrous cementitious materials). The characteristic particle sizes of the slags (i.e., mean, mode, $D_{(v,10)}$, $D_{(v,50)}$ and $D_{(v,90)}$) are presented in Table 2. It is observed that TS2, which contains the highest crystal content, is milled finer than TS1 and TS3 and that TS3 has the coarsest particle size distribution. Nonetheless, the milled slags are used without further mechanical manipulations as it is reported in the literature that the fineness of such slags has slight effects on their reactivity and performance as SCMs [19,20]. Moreover, the milling energy is kept constant to promote comparability for practical purposes.

Table 2. Characteristic particle sizes and true density of treated slags (after milling), cement and quartz.

Materials	Characteristic Particle Sizes (μm)					True Density (g/cm^3)
	Mean	Mode	$D_{(v,10)}$	$D_{(v,50)}$	$D_{(v,90)}$	
TS1: Treated S1	20.9	12.4	1.6	9.1	53.9	2.952
TS2: Treated S2	13.4	5.5	2.1	6.0	23.0	3.656
TS3: Treated S3 (synthetic)	34.5	12.4	1.8	13.6	104.0	3.291
Cement	12.3	14.2	2.0	9.9	25.0	3.125
Quartz powder	9.4	12.4	2.2	7.5	19.4	2.650

The density of the slags was measured via helium pycnometry (AccuPyc II 1340 V1.09 Helium pycnometer), and the results are provided in Table 2. The accurate density values were later used in hydration studies and SEM image analysis for determination of slag degree of reaction (DoR) over time, which is explained in more detail in Section 2.2. The slags were found to have rather different density values. TS1 as the most amorphous sample with the lowest iron oxide content and the highest silica content has a considerably lower density compared to other slags. In addition, TS2 shows the highest density due most likely to its significantly higher crystalline content compared with TS1 and TS3.

CEM I 52.5 N conforming to EN 197-1 [29] specifications was used in this research as the primary binder for the preparation of mortar and paste mixtures produced for slag strength performance assessment and hydration studies. The particle size distribution and true density test results of the cement are presented in Table 2. The chemical and mineral composition of the cement is also provided in Table 3. To establish a basis for assessing the strength performance and reactivity of the slag, quartz powder was used as inert material. Table 2 also contains the characteristic particle sizes and true density value of this material.

Table 3. The oxide and mineral composition of Portland cement.

Oxide/Property	CaO	SiO_2	Al_2O_3	Fe_2O_3	MgO	Na_2O	K_2O	P_2O_5	LOI
Content (%)	60.9	17.6	6.38	3.72	1.5	<0.7	0.307	1.07	1.84
Mineral	C_3S M1	β-C_2S	C_3A cubic	C_4AF	Anhydrite	Calcite	Quartz	Amorphous	
Content (%)	59.1	6.0	5.8	13.4	5.0	4.0	0.5	6.2	

2.2. Methods

2.2.1. Technical Performance Assessment

The treated slags were characterised for their potential in contributing to hydration reactions, the microstructure of the binder and its strength development. The chemical reactivity of the slags in a cementitious environment, their contribution to the evolution of heat of hydration, portlandite consumption, bound water variations, strength development, porosity and microstructure were experimented to reach a comprehensive overview of their properties and assess their viability for being used as SCMs in concrete. In the following sections, the test methods for measurement of each of the above aspects are described.

2.2.2. Chemical Reactivity (R3 Test)

For each slag, the rapid and relevant, reliable (R3) test was carried out as per ASTM C1897 to measure the chemical reactivity of the slag in a reagent system consisting mainly of $Ca(OH)_2$ and H_2O, with addition of $CaCO_3$, K_2SO_4 and KOH to simulate the reaction medium of hydrating Portland cement [30]. This method was initially developed for evaluating calcined clays [31] and was later extended towards other conventionally used SCMs [32,33].

A potassium solution was produced by dissolving 4.00 g of potassium hydroxide and 20.0 g of potassium sulphate in 1.00 l of reagent water. It was then poured into an air-tight container and placed in a storage environment at 40 °C until the temperature was stable. Fesignated amounts of slag, calcium hydroxide and calcite, as shown in Table 4, were weighed on weighing papers. Next, they were combined and mixed until a homogeneous colour was achieved. The dry mixture was stored in an air-tight container in a storage environment at 40 °C until the mixture's temperature was stabilised. The dry mixture of the main ingredients was then mixed with the potassium solution at 1600 ± 50 rpm for 2 min using a high shear blender so that a homogeneous paste was created. The time of start of mixing was recorded as time zero. A 15.0 g freshly made paste specimen was prepared, and the cumulative heat was measured and recorded following ASTM C1897—Method A. Another 15.0 g specimen was cast into a sample container and cured at 40 °C for 7 days, and the bound water content was determined according to ASTM C1897—Method B.

Table 4. Batched masses of R3 mixtures produced for studying the pozzolanic reactivity of the slags.

Slag (g)	$Ca(OH)_2$ (g)	Potassium Solution (g)	$CaCO_3$ (g)
11.12	33.33	59.94	5.56

2.2.3. Hydration Studies

For each slag, a full cement hydration study was carried out as follows. The heat evolution (via calorimetry), microstructural development (via SEM imaging), evolution of the phase composition (X-ray diffractometry), thermogravimetric response (TGA) and porous structure (characterised via MIP) were explored on the paste mixtures shown in Table 5. The control mixture (P_PC) was made with 100% Portland cement and a water-to-cement ratio of 0.40. The three test mixtures (i.e., P_TS1, P_TS2 and P_TS3) were made with 70% Portland cement + 30% slag and a water-to-binder ratio of 0.40. Another reference mixture was produced (P_QP) where 30% of cement was replaced with an inert material (quartz powder). The rationale behind this is to account for the nucleation effects of the slags. Each paste was produced using a high-shear mixer at 1600 ± 50 rpm for 2 min. Samples were cast into 12 ml tubes, sealed and placed in a water bath for curing at 23 ± 2 °C. At each age of testing (1, 7, 28 and 91 days), one tube was randomly taken out and the specimen was ejected from the tube and cut into different slices.

Table 5. Mixing proportions and batching values of paste mixtures.

Paste Label	Slag Source	Mixing Ratios (wt./wt.)		
		Water-to-Binder	Slag-to-Binder	Quartz-to-Binder
P_PC	–	0.4	0.0	0.0
P_QP	–	0.4	0.0	0.3
P_TS1	TS1: Treated S1			
P_TS2	TS2: Treated S2	0.4	0.3	0.0
P_TS3	TS3: Treated S3			

Two slices were dedicated to XRD measurements. One specimen was tested in its freshly cut state, and the other was tested as a powder. The reason for running the XRD test on both fresh and milled specimens is to increase the accuracy of phase quantification. The hydrated phases can be affected during routine XRD sample preparation steps (i.e., hydration stoppage, drying and milling), which might introduce unwanted biases into the measurements [34]. Such phases can better be measured and quantified when exposed to XRD in the fresh state. As such, the surface of the freshly cut specimen was smoothened using 400 grit sandpaper and then flushed with water. The extra water film was removed from the surface, and the specimen was directly subjected to the test. The test conditions are the same as described in Section 2.1. Another sample was prepared for XRD measurement in the dried and milled state for the purpose of more accurately quantifying anhydrous/clinker phases [34]. To this end, the specimens were crushed into pieces and their hydration was stopped following a solvent-exchange protocol. The solvent was then fully removed from the specimens by storing them in a low-vacuum desiccator. They were then milled below 100 µm and exposed to the XRD test. The starting crystal structure data were taken from Snellings (2016) [34]. All structure parameters of the anhydrous phases were fixed at levels obtained from the XRD analysis of anhydrous slags and the cement powder. Rietveld curve fitting was applied to each diffraction pattern in both fresh and milled cases, and the mass attenuation coefficients were calculated using the compositions of the mixtures, taking into account their water content. In the case of fresh specimens, the water content was assumed to be the same as the batched water-to-binder ratio (0.4), and for the milled specimens, only the chemically bound water (measured via thermogravimetric analysis) was taken into account. The corrected mass proportions of the anhydrous phases were extracted from the Rietveld analysis results of the milled specimens, and the fresh specimen results were used for determining the hydrated phases. The results were then combined to determine the evolution of phase composition of the hydrating pastes over time. The Rietveld analysis results were used to determine the clinker degree of reaction (DoR). This was accomplished by proportioning the starting and current combined mass fractions of C_3S, C_2S, C_3A and C_4AF. However, due to the primarily amorphous structure of the slags, determination of their DoR using the Rietveld analysis results was not possible. As such, SEM image analysis was used for estimating the slag DoR over time as a means to evaluate their reactivity. The percentage of slag surface area in the images at a certain age can be compared to its initial value, which can then be used to estimate its DoR.

One hydrated paste slice was dedicated to SEM imaging at each age. For each slag, SEM images were made after 7, 28 and 91 days of hydration. The hydration-stopped slices were impregnated under vacuum using Epofix resin. Impregnated specimens were removed from the mould after 24 h of hardening. The specimens were polished (using a water-free lubricant) with a 9 µm abrasive until the specimen was uncovered while making sure not to expose the non-impregnated portion. Then, the specimens were polished for 2–10 min at 3 and 1 µm until all scratches were removed. The polished surfaces were exposed to scanning electron microscopy, where energy dispersive spectrometry (EDS) and back-scattered electron (BSE) images were acquired and analysed to determine the slag DoR over time. Image data were acquired using FEI FEG Nova NanoSEM 450 equipped with a Bruker XFlash 5030 detector. SEM BSE and EDS mappings were acquired at 500x magnification at an electron acceleration voltage of 20 kV. For each specimen, 25 or 100 BSE

images were taken in a raster of 5 × 5 or 10 × 10, depending on slag type and particle size, such that the images were representative for the sample. The original dimensions of the images were 1536×1024 pixels and were cropped to 1498 × 952 pixels to remove any overlaps on the edges of the neighbouring images. For each specimen, 2–4 EDS mappings were taken, resulting in 21 mappings in total. EDS mappings containing Mg, Al, Si and Ca were combined with BSE images and converted to a colour image. Figure 2a,b shows a sample BSE image and a combined BSE+EDS image, respectively. In Figure 2b, the colours red, green and blue indicate Si, Mg and Ca, respectively. Regions containing both Si and Mg are shown as orange. The images were processed using a procedure that applies neural networks with the aim of segmentation such that all slag particles are selected without selecting other phases/areas.

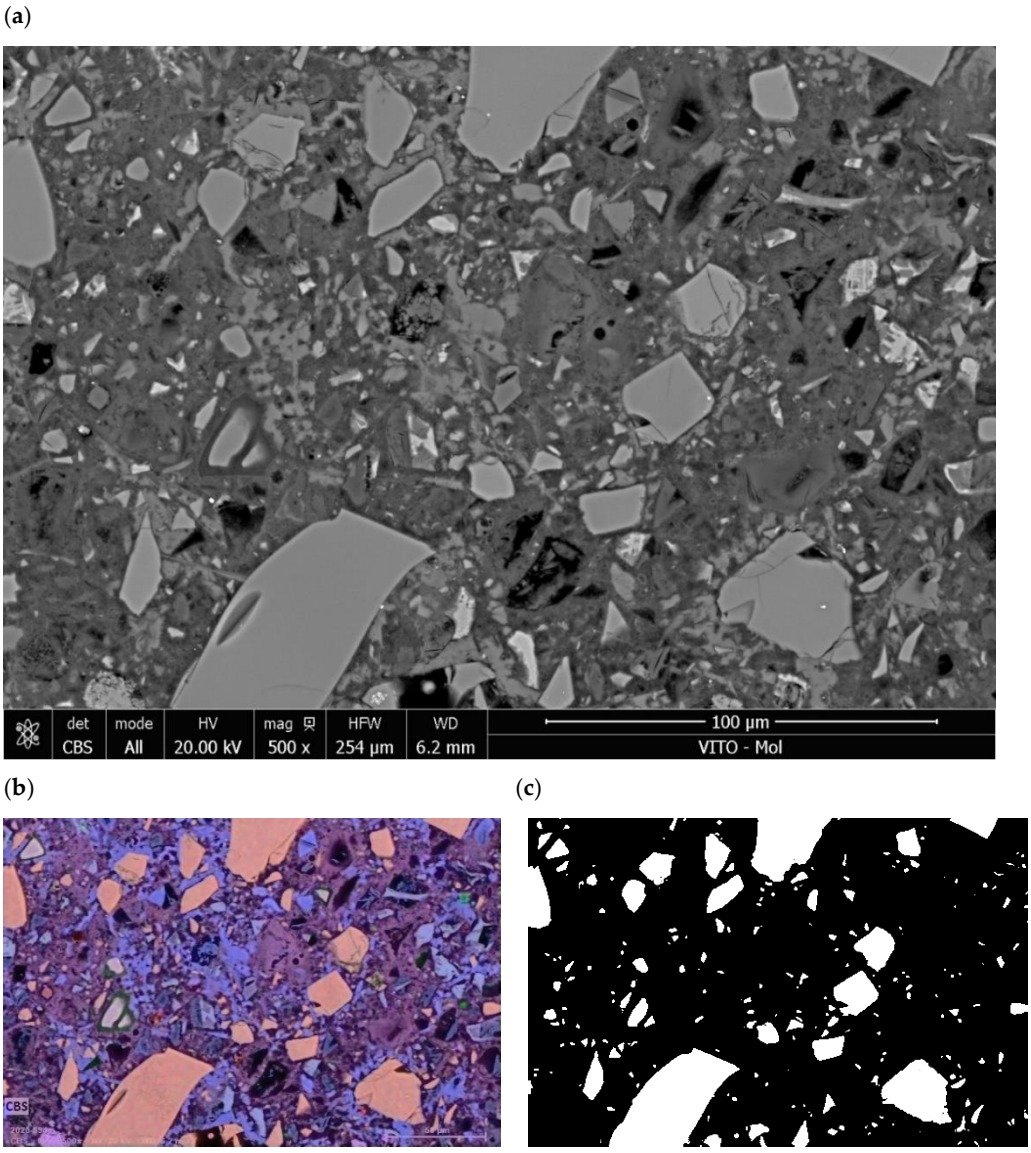

Figure 2. Sample raw and processed images. (**a**) BSE image, (**b**) combined BSE+EDS image and (**c**) segmented image.

The model used was a U-net developed by Ronneberger et al. (2015) [35]. To create training data for training the model, the 21 combined EDS+BSE images were manually segmented using thresholds and filters as follows. First, a threshold was applied to the BSE images to select only the brightest phases, and the noise was removed. This selected mainly the slag and clinker phases. Next, for each selected particle, the average value of the EDS

mappings was calculated and a K-means algorithm was applied to select the cluster of EDS values that consisted of slag. Then, the segmented images were manually adapted to come to an optimal segmentation. Figure 2c shows a sample segmented image. The resulting segmentations were paired with the respective BSE images and used for training the model. Nineteen BSE images were used for training the model and two for testing. Training was carried out by transfer learning for 300 epochs on one NVIDIA GeForce RTX 2080 Ti GPU. The model was then applied to the test set. The average difference between the model output and the test label was 5.95%, and the average difference between the surface area of slag was 1.55%. After training, the model was used to segment all BSE images. Using the mixture batching proportions (Table 5) and the density of different ingredients (Table 2), the average expected initial slag surface area ratio in the polished sections was calculated. Then, the model results were used to calculate the average surface area ratio of slag grains over time and the variations were converted to the degrees of reaction.

The bound water and portlandite contents of the paste mixtures were measured via thermogravimetry in order to assess the progress of hydration reactions and portlandite generation/consumption. Representative hydration-stopped milled specimens were heated at a 10 °C/min rate from 30 °C up to 1000 °C under a nitrogen atmosphere at a 50 mL/min flow rate. The bound water was determined by measuring the mass change between 50 and 550 °C, and the portlandite content was estimated as the mass loss between 400 and 500 °C using the tangential method.

Finally, one slice was subjected to mercury intrusion porosimetry (MIP) for characterising the pore structure evolution over time. Using a mercury porosimeter model Pascal 240 Series (Thermo Fisher Scientific, Waltham, MA, USA), 0.3–0.4 g of hydration-stopped specimens was placed in sample chambers and an initial pressure of 14.0 Pa was applied to fill the void spaces in the specimens. After reaching equilibrium, the mercury pressure was slowly increased up to 200 MPa and the pore size distribution and characteristic parameters were determined using the intruded mercury volume at each pressure level, assuming a cylindrical model for the pore structure.

2.2.4. Mechanical Performance (Strength Activity and Strength Development)

To assess the cementitious performance of the slags, a set of mortar mixtures with and without replacement of cement with slag was produced following EN 196-1 [36] guidelines. Table 6 summarises the batched masses of different ingredients for the production of each mortar mixture. The reference cement mortar mixture (labelled M_PC) was composed of Portland cement, water and standard CEN reference sand with a water:cement:sand ratio of 1:2:6. In the case of test mixtures, 30% of the cement (by mass) was replaced by each of the three slags (labelled as M_TS1, M_TS2, M_TS3) to investigate the influences of such replacements on the flowability (measured in accordance with EN 1015-3 [37]), compressive strength and flexural strength of the mortars (as per EN 196-1).

Table 6. Batched masses of produced mortar mixtures for strength activity and strength development tests.

Mortar Label	Slag Source	Batched Masses for Preparation of Mortars (g)				
		Cement	Slag	Quartz	Water	Sand
M_PC	–	900	–	–	450	2700
M_QP	–	630	–	270	450	2700
M_TS1	TS1: Treated S1					
M_TS2	TS2: Treated S2	630	270	–	450	2700
M_TS3	TS3: Treated S3 (synthetic)					

A second control mortar mixture was produced where the 30% replacement of cement was done using quartz powder as an inert material to account for the filler effect of the slags (mixture referred to as M_QP). Each mixture was produced four times (one batch for each testing age: 1, 7, 28 and 91 days), cast into three 40 × 40 × 160 mm^3 prismatic moulds, covered with plastic sheets and stored at 20 ± 2 °C for 24 h. Next, the specimens

were removed and cured in a climate chamber at 20 ± 1 °C and RH > 95% until the age of testing. Upon curing, the specimens were first tested for their flexural strength, and the broken halves were then exposed to a compressive strength test.

2.2.5. Environmental Performance Assessment

The leaching behaviour of the hydrated cement mortar mixtures (produced as per Table 6) is characterised as per the EN 12457-4 [38] standard test method in order to monitor the leaching of ions and heavy metals for the simulated end-of-life mortars containing such slags. After preparing and curing the mortars for 91 days, they were crushed using a jaw crusher to <10 mm and dried in an oven at 80 °C for 24 h. Following the standard test method, 90.0 g of a representative sample of the crushed mortar was added to 900 mL of deionised water and stirred for 24 h. A representative sample was then taken from the eluate, and the electrical conductivity (EC) and pH of the eluate were measured with a Multimeter Seven Excellence instrument. The concentration of the dissolved metals in the eluates was measured via ICP-AES.

2.2.6. Standards and Limitations

While there are no standards specifying mechanical performance requirements for non-ferrous metallurgical slags as SCMs, EN 15167 [39] requires a minimum 28-day strength activity index (SAI) of 70% when 50% of the cement is replaced by ground granulated blast furnace slag. Despite the substantial differences in the source and composition of the slags studied in this research with ground granulated blast furnace slag (GGBFS) generated in pig iron production, such a criterion appears a reasonable minimum requirement for SCMs used in concrete and is thus adopted here as the minimum SAI for assessment of the slags. In addition, there are no requirements yet set forth for the R3 test results of SCMs (i.e., 7-day heat release or bound water). The R3 results of the slags were compared with those of few conventional SCMs (GGBFS, coal fly ash and calcined clay) and a typical quartz powder to put the values in prospective.

For the evaluation of environmental performance, the limitations set forth by the Flemish legislation VLAREMA (17 February 2012—Order of the Government of Flanders adopting the Flemish regulation on the sustainable management of material cycles and waste) for the use of waste as resources in construction applications were used. The heavy metal leaching limitations are provided along with the results for each slag later in the Section 3.

3. Results

3.1. Technical Performance Results

3.1.1. Chemical Reactivity

The R3 test results, including the 3- and 7-day heat release and the 7-day bound water values for the three slags, are reported in Table 7. The heat release patterns of the three slags are also shown in Figure 3. The heat release and bound water values of three conventional SCMs (typical samples of GGBFS, coal fly ash and calcined clay) are also given in Table 7 for comparison. Note the reported values for a fully inert material such as quartz and compare them with those of the slags in this study. While the reactivity of the slags was evident, they did not appear to be reactive when comparing the heat release and bound water values with those of the blast furnace slag or calcined clay. Nevertheless, the slags showed comparable heat release and bound water values with respect to the selected coal fly ash.

Table 7. R3 test results for the slags, along with some conventional SCMs and inert quartz.

Slag Source	3-Day Heat (J/g SCM)	7-Day Heat (J/g SCM)	7-Day Bound Water (g/100 g Dried Paste)
TS1: Treated S1	58.0	104	3.2
TS2: Treated S2	58.0	88.0	2.3
TS3: Treated S3 (synthetic)	73.0	127	3.3
Some conventional SCMs			
Blast furnace slag	460	518	8.5
Fly ash	104	173	4.5
Calcined clay	527	574	10.4
Inert material			
Quartz	16	21	1.3

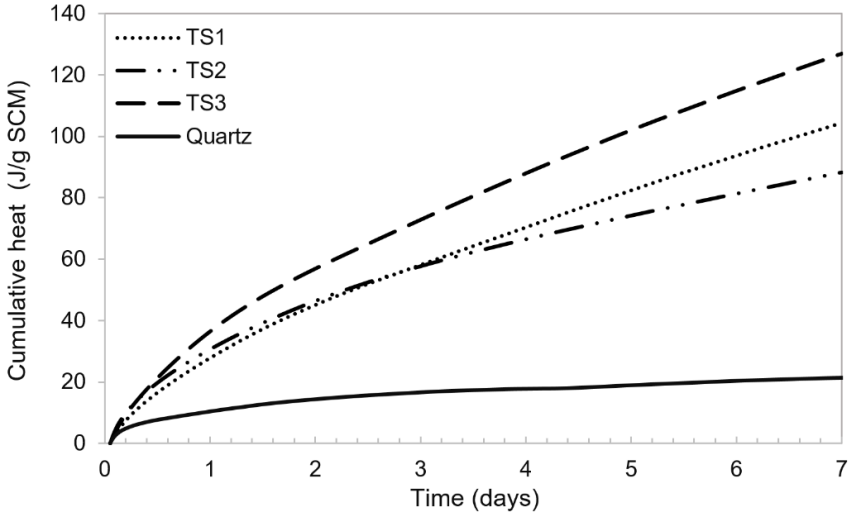

Figure 3. Heat release patterns of the treated slags and quartz as per the R3 test.

3.1.2. Calorimetry

The specific heat flow and cumulative heat of the pastes produced with and without slag in the first 72 h and up to 28 days are shown in Figure 4a,b, respectively. It was observed that the heat flow normalised per gram of cement in the case of P_PC was similar to the pastes blended with slag up to 15 h from the time of mixing, after which the mixtures incorporating slag showed a higher rate of heat flow. The mixture containing quartz powder also showed a higher heat flow rate compared to the pure cement paste at all times and also compared to the slag-blended pastes up to the age of 3 days (except for short time intervals where it falls below). There was no significant shift in the heat flow peak times of the slag-blended mixtures in either direction compared to that of Portland cement. In the case of the quartz-blended mixture, however, the peak time slightly shifted to the left (indicating faster early-age hydration reactions), which could be the result of the nucleation effect of quartz powder or the higher access of the cement to water (higher w/c ratio compared to the control), which could expedite the hydration. In other words, since unlike the slags, the quartz had no retarding effect, the heat flow rate peaked at an earlier time. Moreover, the flow rates were higher in the first 11 h in the case of the mixture containing quartz powder compared to slag-blended mixtures. Similar retardation effects were reported by Feng et al. for copper slag [16]. Nonetheless, the heat release behaviour of all mixtures containing slags were similar and close to that of the mixture containing quartz, and no significant difference in the cumulative heat flow of such mixtures was observed up to 28 days (see Figure 4). This also signifies the poor pozzolanic reactivity of the treated NFM slags compared to other SCMs such as GGBFS, silica fume and calcined clays.

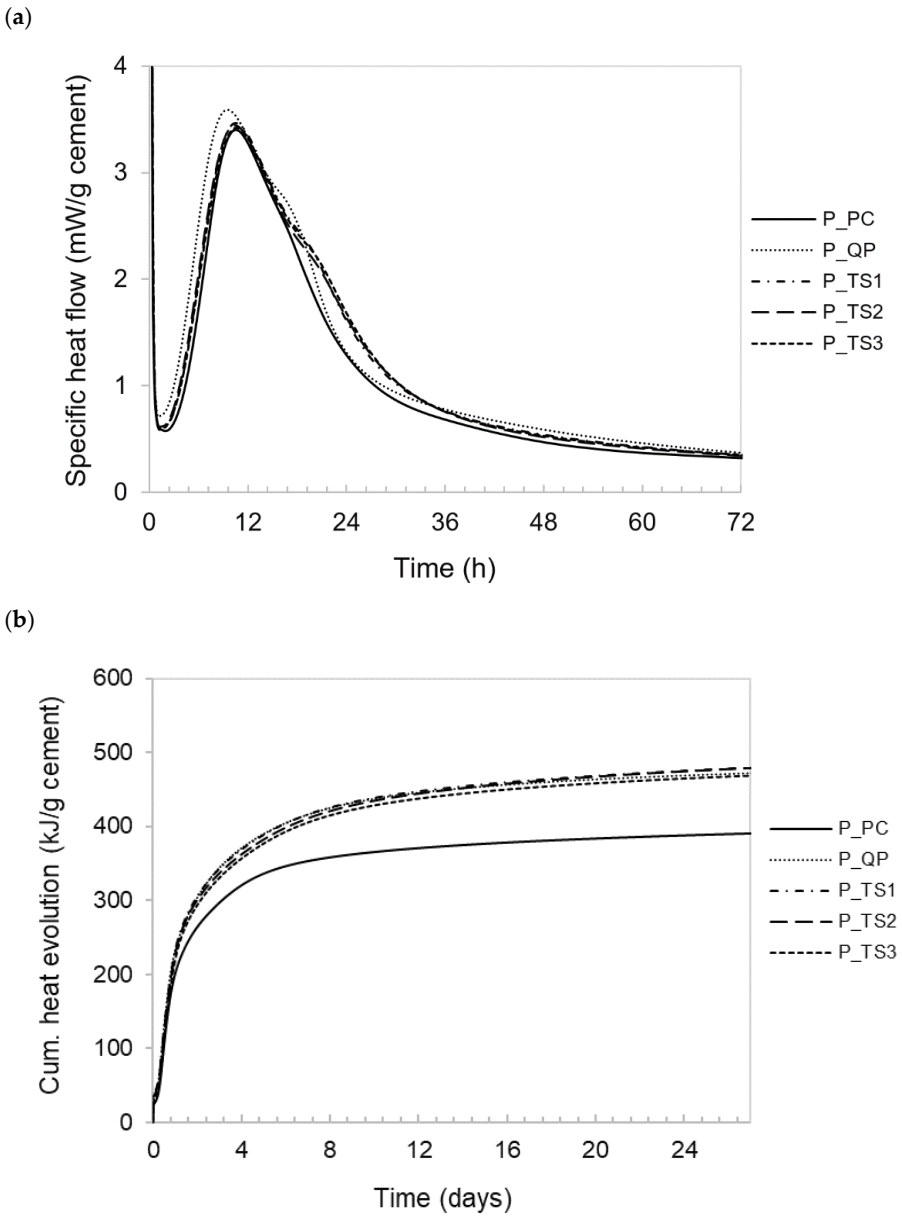

Figure 4. The specific heat flow and cumulative heat patterns of the pastes per gram of cement (**a**) in 24 h and (**b**) in 7 days.

3.1.3. Phase Evolution

Figure 5 shows the XRD patterns of the different pastes over time. It was observed that in all pastes, there was a quick decline in the clinker phases (C_3S, C_3A and C_4AF), while hydrates (portlandite, ettringite, hemicarboaluminates and monocarboaluminates) were formed. Note that similar hydration products were formed in all pastes. The Rietveld analysis results are plotted in the form of area charts in Figure 6a–e. Comparing the rate of consumption of the clinker phases between P_PC and other pastes, it can be concluded that the clinker reactions progress faster in the blended mixtures. The calcite also appeared to be consumed over time in all mixtures, and hemicarboaluminate and monocarboaluminate phases formed at day 1 and continued to slightly grow over time. The P_TS2 paste showed some traces of fayalite, which comes from the slag. However, the fayalite did not appear to be reacting.

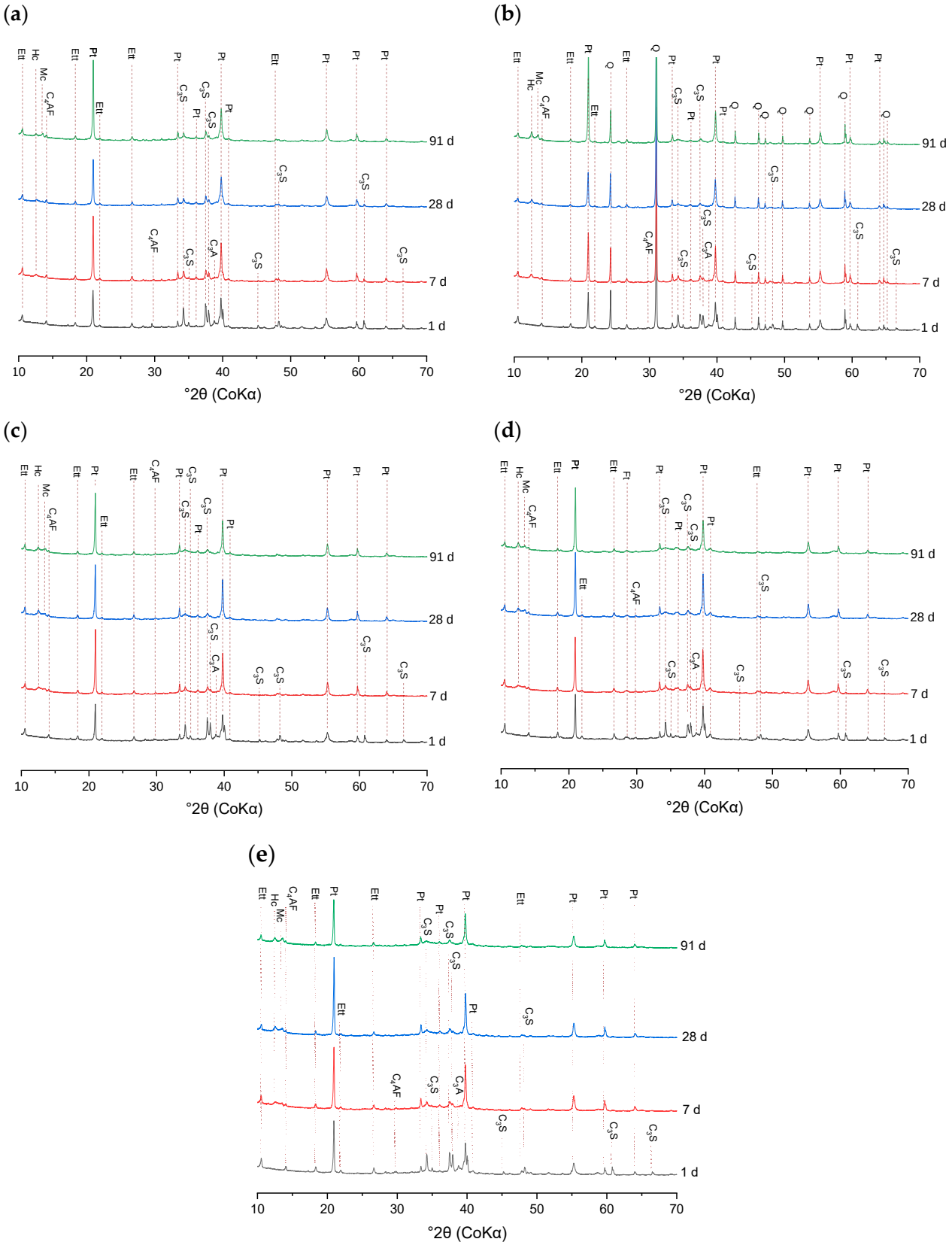

Figure 5. The evolution of X-ray patterns of different pastes over time: (**a**) P_PC, (**b**) P_QP, (**c**) P_TS1, (**d**) P_TS2 and (**e**) P_TS3. Ett: ettringite; Hc: hemicarboaluminate hydrate; Mc: monocarboaluminate hydrate; Pt: portlandite; Ft: fayalite.

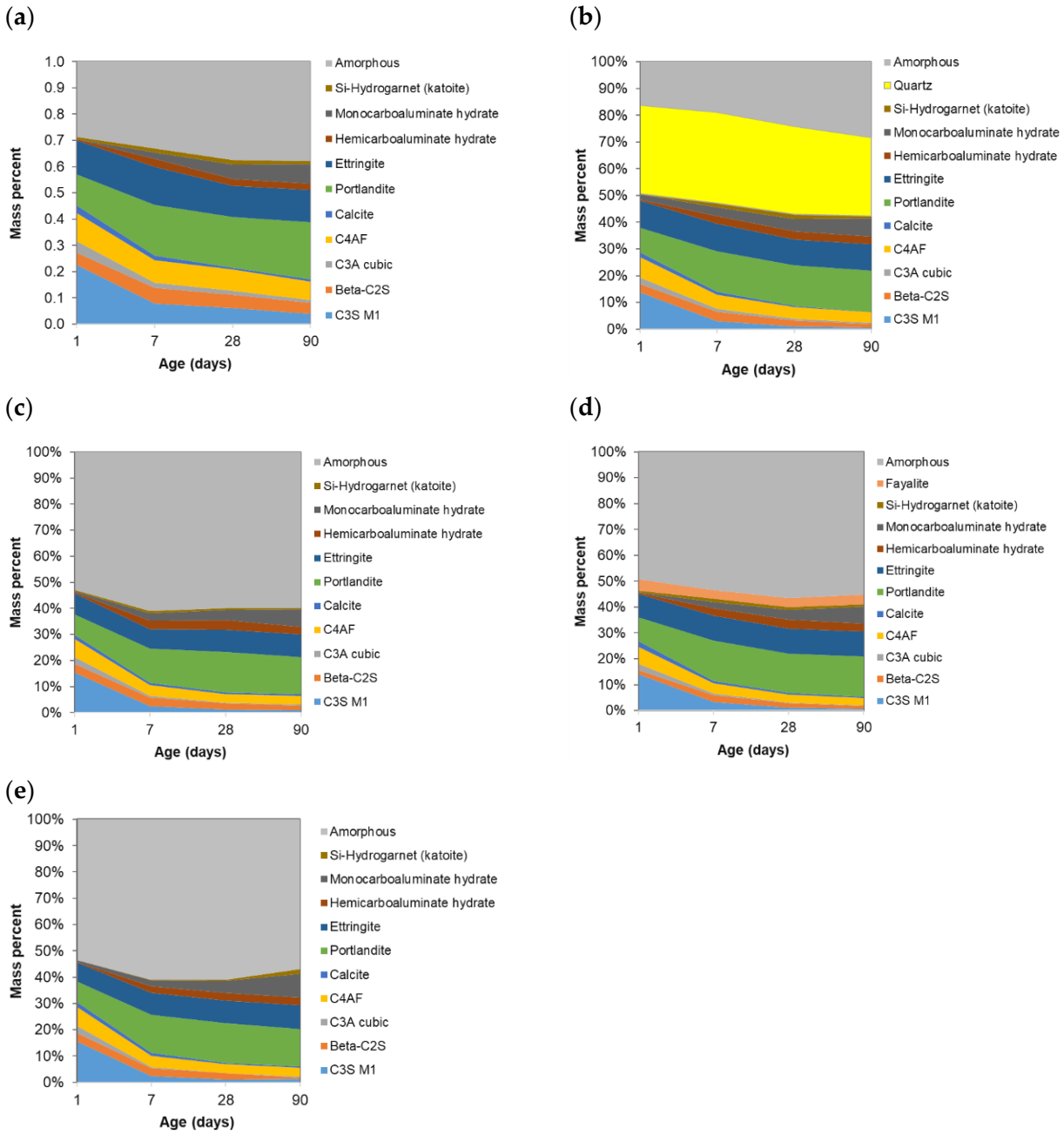

Figure 6. Area charts displaying the evolution of different phases over time; values in g/100 g of binder. (**a**) P_PC, (**b**) P_QP, (**c**) P_TS1, (**d**) P_TS2 and (**e**) P_TS3.

Figure 7 shows the clinker DoR for different pastes over time. Note that the clinker degree of reaction of the blended pastes were in all cases and ages higher than that of pure cement paste (P_PC). One reason for the higher DoR in blended pastes is the replacement of part of the cement with an inert (quartz) or a moderately reactive material (slag), which resulted in an increase in the effective water-to-cement ratio. As such, the accessibility of water for cement was enhanced, leading to more reactions at any given time. Comparing the three slags with each other, it could be argued that the mixture containing TS2 experienced a slightly higher clinker reaction compared to TS1 and TS3. Nevertheless, all three slags were almost equally reactive, judging by the calorimetry and clinker DoR results.

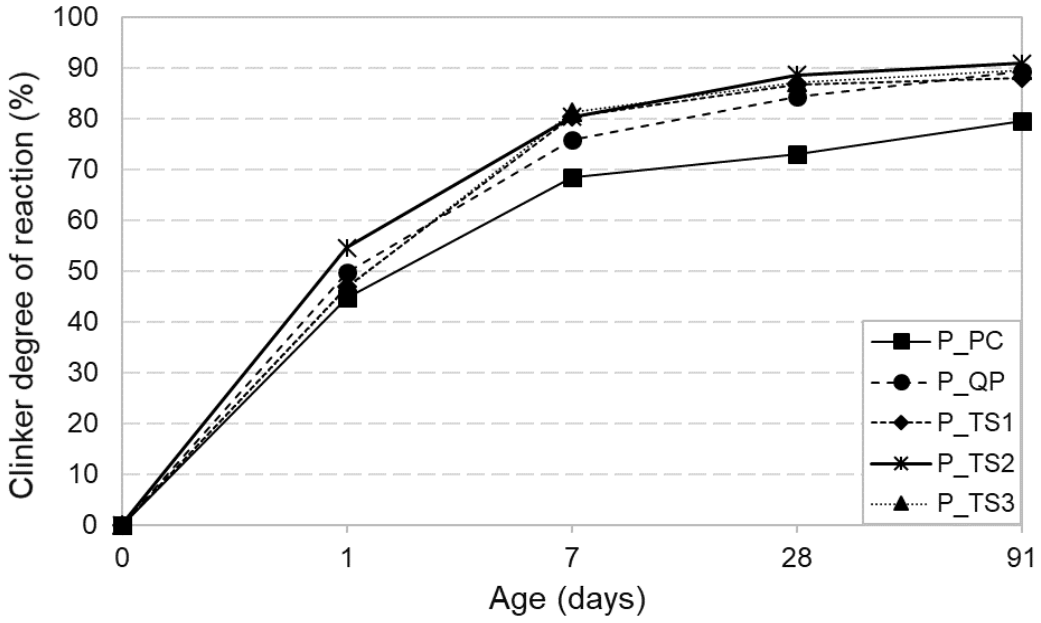

Figure 7. The clinker degree of reaction in different pastes up to the age of 91 days.

3.1.4. Thermogravimetry

The bound water contents of the pastes up to the age of 90 days are plotted in Figure 8a. It was observed that the bound water values (per 100 g of cement) for the three pastes incorporating slag were similar up to the age of 90 days and higher than those of pure Portland cement paste, especially at later ages. They were also lower than those of the quartz-blended mixtures (especially at 1 day). The higher bound water content of the blended pastes compared to the pure cement paste is an indication of the availability of more water for cement hydration (due to the replacement of part of the cement with the slags/quartz). However, comparing the 1-day bound water of the slag-blended pastes with that of the pure Portland cement paste and the paste containing quartz indicates the presence of a retardation effect by the slags. This could probably be due to the presence of heavy metals such as lead and zinc, which have previously been reported to have a retardation effect on cement hydration [40–42].

The portlandite contents of the pastes up to the age of 90 days are plotted in Figure 8b. It was observed that the portlandite content of the blended pastes were higher than that of pure Portland cement paste at all ages, which is an indication of more hydration reactions (due to the availability of more water for cement reactions). This is in agreement with the bound water results. However, except for the age of 1 day, the slag-blended pastes appeared to have formed equal or higher portlandite contents compared to the paste incorporating quartz.

3.1.5. SEM Image Analysis

The calculated DoR values over time are plotted in Figure 9, along with the corresponding standard errors. It was observed that at 7 days, the average DoRs were still quite low and comparable to the error margins. It can thus be concluded that up to 7 days, the slag particles do not react significantly. However, DoR values of 20% to 30% were measured for 91-day samples. This is in alignment with the compressive strength results where no contribution to strength was observed for all three slags at early ages, while the slags showed some strength activity at later ages.

(**a**)

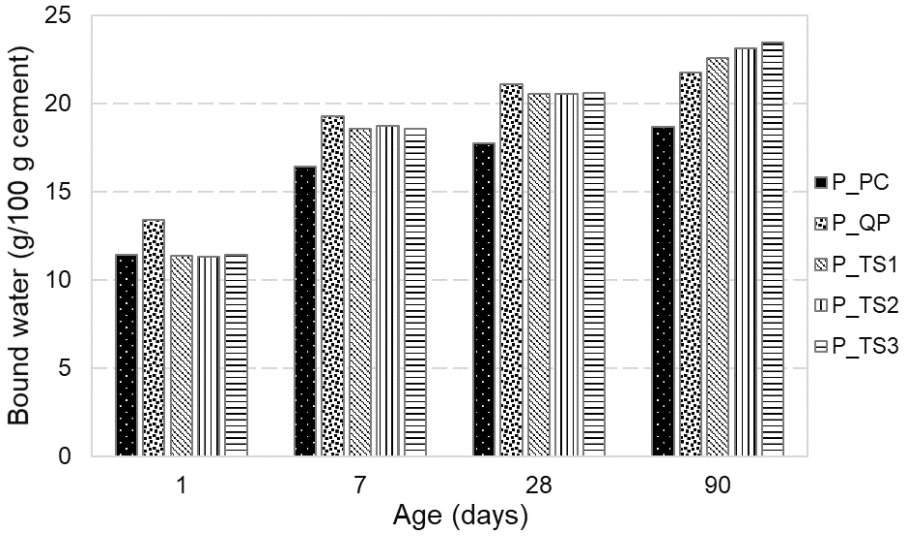

(**b**)

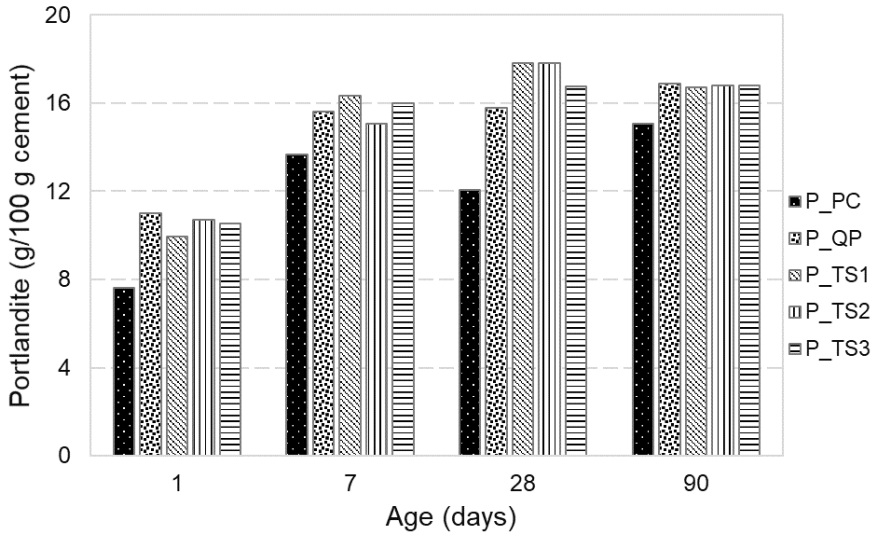

Figure 8. The bound water (**a**) and portlandite (**b**) contents of the paste mixtures up to the age of 90 days.

3.1.6. Porosimetry

The pore structure of the hydrated paste mixtures (per Table 5) was characterised using mercury intrusion porosimetry with the aim of learning more about the effects of partial replacement of Portland cement with the studied slags. Figure 10a,b shows the pore volume of the pastes as a function of the pore entry diameter for the 28- and 90-day old samples, respectively. Figure 10a clearly indicates that the partial replacement of Portland cement with either slag type or quartz powder resulted in both coarsening of the pore structure and increase in porosity up to the age of 28 days. However, a considerable refinement took place in the slag-blended mixtures at later ages, resulting in a decrease in their porosity and pore size parameters, while the mixture containing quartz powder (P_QP) experienced significantly less refinement in pore structure between 28 and 90 days. The pore structure parameters of the 28- and 90-day pastes are tabulated in Table 8. It was observed that the slag-blended mixtures had lower porosity compared to P_QP both at 28 days (despite their coarser particle size according to Table 2), and the difference became

more pronounced by the age of 90 days. This can be interpreted as the long-term reactivity of the slags as cementitious materials. The least refinement between 28 and 90 days took place for P_TS2, which could be associated with the considerably higher crystalline content of TS2 compared to TS1 and TS3.

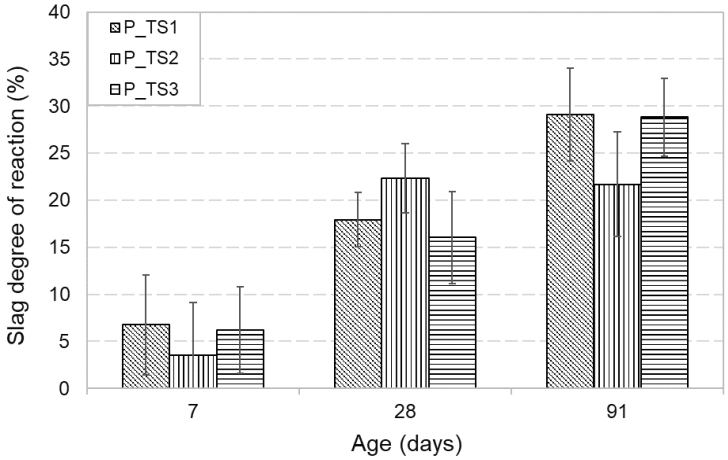

Figure 9. The slag degree of reaction in different slag-blended pastes up to the age of 91 days.

(**a**)

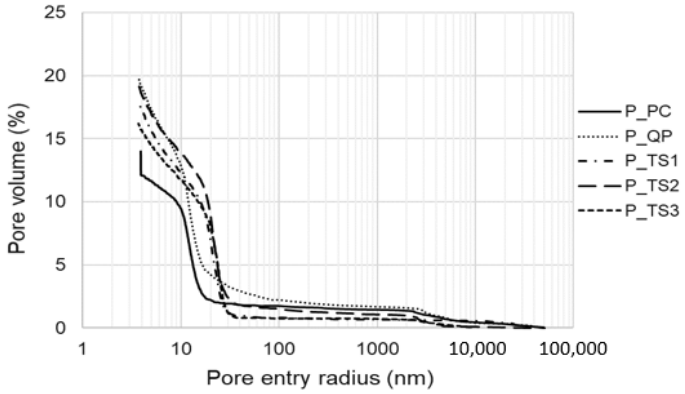

(**b**)

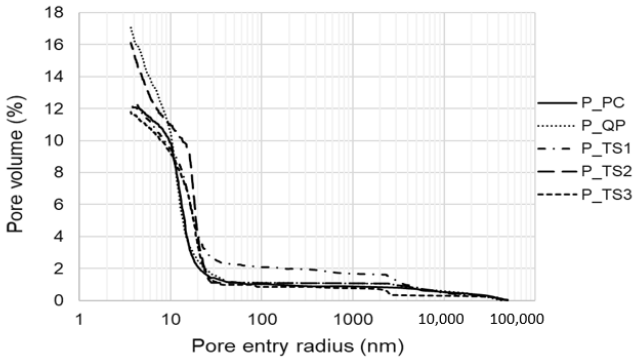

Figure 10. Pore volume of paste mixtures as a function of intruded pore diameter (**a**) at 28 days and (**b**) at 90 days.

Table 8. Characteristic pore structure parameters of the hardened paste mixtures at 28 and 90 days.

Parameter	P_PC (28 days)	P_QP (28 days)	P_TS1 (28 days)	P_TS2 (28 days)	P_TS3 (28 days)	P_PC (90 days)	P_QP (90 days)	P_TS1 (90 days)	P_TS2 (90 days)	P_TS3 (90 days)
Total cumulative volume (mm^3/g)	71	114	105	107	94	70	96	67	86.5	58
Total specific surface area (m^2/g)	16.3	24.4	20.1	19.5	16.6	12.9	21.4	11.1	17.3	9.5
Average pore radius (nm)	11.9	11.9	17.5	19.0	19.9	12.9	11.2	16.1	16.9	16.6
Total porosity (%)	13.9	20.1	18.0	19.2	16.2	12.7	16.9	12.4	16	11.7
Threshold pore entry radius (nm)	15.9	17.4	27.0	25.8	28.3	18.1	17.0	23.0	1.85	23.9
Critical pore entry radius (nm)	12.7	12.5	22.0	21.9	23.2	12.7	12.1	16.5	2.20	18.5

3.1.7. Mechanical Performance

The flowability and the 1-, 7-, 28- and 91-day compressive and flexural strength results of the mortar mixtures are shown in Table 9. An important observation was the increase in the flowability by replacement of cement with slags, which is favourable from a practical point of view. This is mainly due to the coarser particle size (in the case of TS1 and TS3) and less reactivity of the slags compared to Portland cement.

Table 9. The flowability, compressive and flexural strength of the mortar mixtures.

Mortar Label	Flow (%)	Compressive Strength (MPa)				Flexural Strength (MPa)			
		1 Day	7 Days	28 Days	91 Days	1 Day	7 Days	28 Days	91 Days
M_PC	81.5	24.9 ± 0.6	56.6 ± 1.0	65.1 ± 1.0	69.3 ± 0.9	6.5 ± 0.3	10.5 ± 1.2	11 ± 0.3	13.0 ± 2.0
M_QP	91.0	12.6 ± 0.4	36.5 ± 1.1	49.0 ± 1.3	55.8 ± 3.0	3.1 ± 0.1	7.0 ± 0.3	7.4 ± 0.2	8.8 ± 0.4
M_TS1	95.5	11.8 ± 0.1	37.7 ± 0.6	46.2 ± 1.1	53.3 ± 1.0	4.1 ± 0.2	8.7 ± 0.6	9.3 ± 0.8	10.9 ± 0.9
M_TS2	106	10.5 ± 0.1	36.8 ± 0.4	47.7 ± 1.2	55.5 ± 0.9	3.5 ± 0.1	8.1 ± 0.2	9.4 ± 0.7	9.9 ± 0.5
M_TS3	98.5	12.3 ± 0.2	39.4 ± 0.4	47.5 ± 0.8	53.6 ± 1.2	4.1 ± 0.2	8.8 ± 0.5	9.6 ± 1.8	10.2 ± 1.6

The compressive and flexural strength results are plotted in Figure 11 as well. It is observed that all mixtures containing slag gained less strength compared to both P_PC up to the age of 91 days. However, the strength ratios were found to continuously increase over time. The strength activity index (SAI) values are reported in Table 10, which suggest that the strength gain in 1 day in the case of all slags was less than 50% of the control mixture, while that of the P_QP mixture was 50%. This is an indication of the retarding effect of the slags on cement hydration and early-age strength development. This confirms the TGA findings on the pastes at 1 day. The P_QP paste developed more bound water (see Figure 8a) and generated slightly more heat (see Figure 4a) compared to P_TS1, P_TS2 and P_TS3. Nonetheless, the compressive strength values of slag-blended mixtures reached 65–70% of the reference mortar at 7 days, which suggests the later-age reactivity of the slags. The 28-day strength values, which are benchmarks for the assessment of the performance of slags as SCMs, were all similar and slightly above 70%. As such, all slags met the minimum 28-day SAI requirements of EN 15167/EN 450-1.

In comparison with P_QP, it is worth noting that while the slag-blended mixtures showed similar compressive strength results at 1 day, they slightly exceeded the compressive strength of Q_QP at 7 days. This is in agreement with the calorimetry findings (Figure 4a). It was observed that P_QP initially showed a higher rate of heat flow up to 19 h and then fell below the slag pastes up to the age of 3 days. This might account for the strength development pattern of slag pastes compared to P_QP. Similar strength values compared to slag-blended mixtures were observed for P_QP at later ages. Interestingly enough, P_QP showed lower flexural strength values compared to slag mixtures at all ages. The reason behind the generally higher compressive strength of P_QP compared to slag pastes (despite the higher reactivity of the slag) and its lower flexural strength could have to do with the higher mechanical strength of quartz and its lower chemical reactivity compared to the slags, respectively. As shown in Figure 1, granulation of the slags resulted in the amorphisation of their mineral structure. Test results were also indicative of the fact that such amorphisation further reflected itself in the density of the slags as well. The same slags slowly cooled in air were found to have density values of 3.23, 3.78 and 3.65 kg/m^3, which were considerably higher than those of the granulated slags used in this research (see Table 2). The amorphisation of the microstructure resulted in increased entropy, which often translates to lower mechanical strength. This was while P_QP contained fully crystalline quartz particles that better resist compressive loading compared to granulated slags. Due to the chemically inert nature, however, quartz cannot form chemical bonds with the surrounding cement matrix and thus acts as a point defect at the bottom half of the bending specimen (i.e., the tensile region), causing failure at lower stress levels. In the slag-blended mixtures, in contrast, the formation of hydration products at the interface between slag

grains and the surrounding paste could contribute to the tensile and thus flexural strength of the mixtures at any age. This could explain why slag-blended mixtures showed lower compressive strength but higher flexural strength compared to Q_QP.

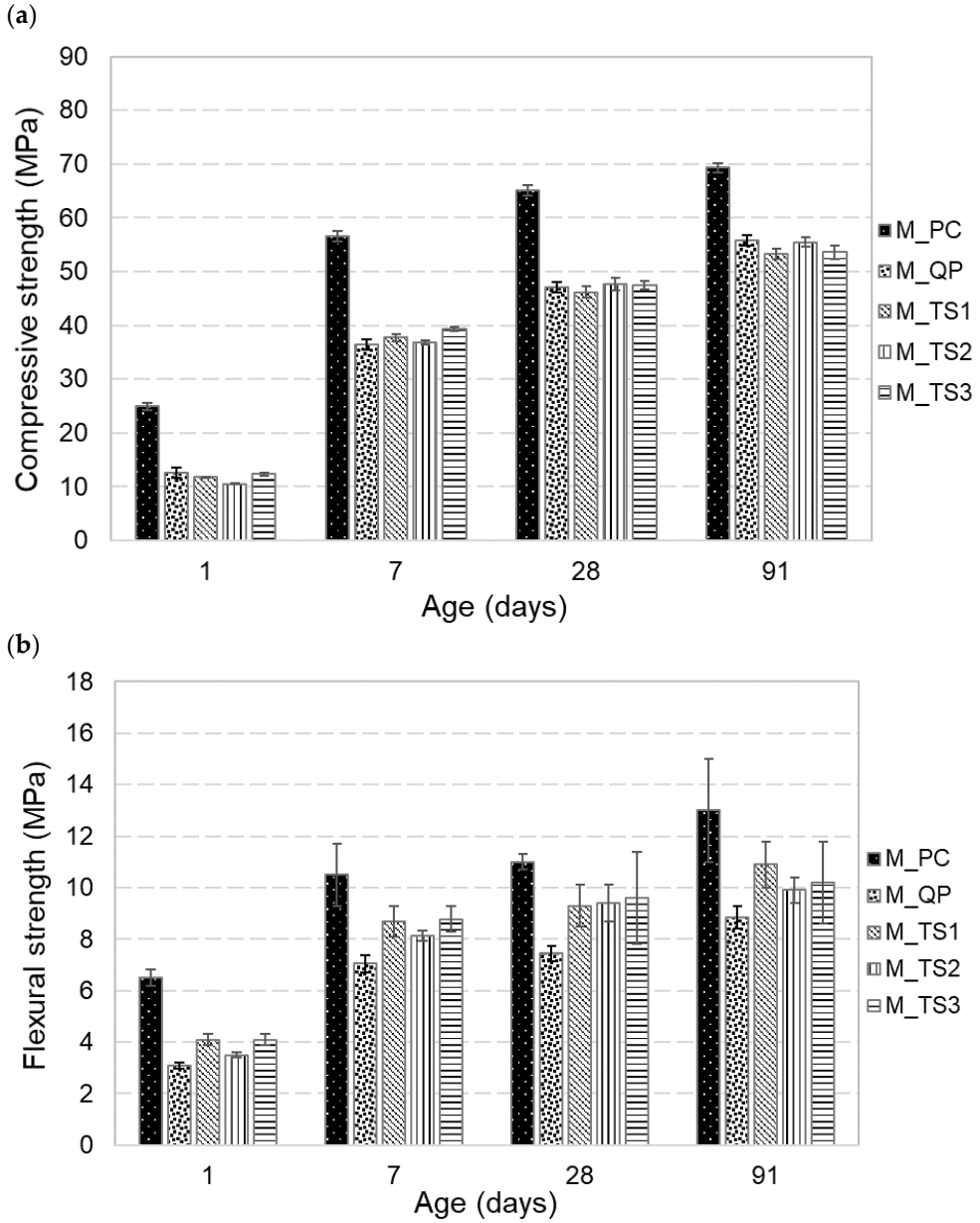

Figure 11. Compressive and flexural strength results of mortar mixtures up to the age of 91 days. (**a**) compressive strength, (**b**) flexural strength.

Table 10. Strength activity indexes (SAIs) of the slags at different ages.

Mortar Label	Slag Source	SAI at Different Ages (Days)			
		1	**7**	**28**	**91**
M_QP	–	0.50	0.64	0.75	0.81
M_TS1	TS1: Treated S1	0.47	0.67	0.71	0.77
M_TS2	TS2: Treated S2	0.42	0.65	0.73	0.80
M_TS3	TS3: Treated S3	0.49	0.7	0.73	0.77
Standard limitation	EN 15167	–	–	0.70	–

3.2. Environmental Performance Results

Table 11 shows the leaching results. The leaching values were in all cases below the standard limitations. The only exception was chromium leaching for TS1. No other significant difference was found between the leaching behaviour of the mixtures containing different slags. It can thus be concluded that the slag treatment sufficiently removed the heavy metals from the slags.

Table 11. The batch-leaching test result of the crushed mortar mixtures: metal content is expressed in mg/kg dry-mass basis.

Mortar Label	Slag Source	As	Ba	Cr	Pb	Zn	Sb	Ni
M_PC	–	<0.15	13	0.2	<0.1	<0.1	<0.2	<0.05
M_TS1	TS1: Treated S1	<0.15	15	0.52 *	<0.1	<0.1	<0.2	<0.05
M_TS2	TS2: Treated S2	<0.15	12	0.29	<0.1	<0.1	<0.2	<0.05
M_TS3	TS3: Treated S3	<0.15	20	0.16	<0.1	0.1	<0.2	<0.05
VLAREMA limits		0.8	20	0.5	1.3	2.8	1	0.75

* Exceeding the standard limitation.

4. Discussion

In contrast to GGBFS, non-ferrous metallurgical slags are not widely adopted as supplementary cementitious materials for the production of cement-based materials. This could, for the most part, be due to the presence of toxic elements and corrosive anions, leading to environmental concerns and long-term damages to the host concrete member. The low reactivity of such slags, mostly due to their chemistry (high iron oxide and low calcium oxide and alumina contents) and their mineralogy (crystalline oxides and iron silicates), would also make such slags less obvious candidates for use as SCMs. The above reasons make the application of a high-temperature metallurgical treatment prudent for the recovery of valuable metals and the reduction/removal of other heavy metals from slag. Incorporation of calcareous and aluminous additives to slag in the course of thermal treatment to modify the chemistry and the application of rapid cooling can promote the reactivity of the slag to a large extent. Nevertheless, the reactivity of the treated slag can vary across a wide range. Spooren et al. [43] concluded that slags generated from lead, copper and zinc production have been widely studied in the literature as SCMs with strength performance levels ranging from those of an inert filler to exceeding those of typical coal fly ash. In the case of slags studied in this research, it was clearly shown that they have poor/mild pozzolanic performance evidenced by (1) the similar bound water and heat release patterns of the slag-blended pastes and the pastes blended with quartz powder, (2) a lack of significant reactions up to 7 days according to SEM image analysis results, and (3) the low strength activity indexes.

In comparison with the reactivity results reported in the literature for similar non-ferrous slags, the slags studied in this research (real and synthetic) showed rather low reactivity. Sivakumar et al. [21] reported a comparable R3 bound water content for a similar ferro-silicate slag (3.5 g/100 g of SCM) but a considerably higher strength activity index at all ages (74%, 84% and 88% at 7, 28 and 91 days, respectively, for a slag with similar fineness, 92% amorphous content and 3.9% CaO, 11% Al_2O_3 and 32.3% SiO_2). Hallet et al. [20] reported an R3 7-day cumulative heat release in the range of 200–240 J/g SCM for NFM slag with Blaine fineness of 4500–6500 cm^2/g, which is higher than the heat release values observed for TS1–TS3. In comparison to TS1–TS3, the slags used in their study contained high iron oxide and low silica content, more calcium oxide (15–20 wt.%), less alumina content, equal or less amorphous content and slightly higher fineness (especially compared to TS3).

Given the higher reactivity reported by Hallet et al. despite high iron oxide and low silica contents, and also the fact that the rather wide variations in the iron oxide and silica contents in TS1–TS3 did not cause much change in reactivity, it could probably be argued that these two elements are not the primary factors influencing reactivity. For

instance, TS2 contained comparable calcium oxide and higher alumina, similar fineness and similar amorphous content with respect to the slags studied by Hallet et al. but showed lower reactivity.

It is thus not clear how the presence of different oxides contributes to the reactivity and bound water of the slags and their strength performance. As such, a full correlation matrix was developed to see the correlation coefficient between all pairs of oxide content with the R3 7-day heat release and bound water content and the 28- and 91-day strength results for the three studied slags. It should be noted that all slags performed rather similarly in terms of chemical reactivity and strength activity; therefore, the established correlations may not be easily extrapolated to a broader scope of materials covering a wider variation in reactivity. In addition, since the number of studied compositions is low (i.e., 3), the *p*-value of the obtained correlation coefficients should be calculated accordingly, taking into account the low number of observations. A *p*-value lower than 0.1 is considered a signal for the presence of a potentially meaningful correlation between the two parameters. In this regard, no significant correlation was observed between the 7-day cumulative heat release and the FeO, SiO_2 and CaO contents of the slags. The CaO content of the slags was found to directly correlate with the 28-day and especially the 91-day compressive strength of the mortars (r = 0.998; *p*-value = 0.04). MgO also seemed to inversely affect the 7-day heat release (r = 0.991; *p*-value = 0.09). However, no significant correlation was observed between the MgO content and strength development. K_2O and SO_3 were also found to be directly correlated, with both inversely affecting the 28-day compressive strength.

Although a one-to-one correlation between the R3 test and the strength development results was not identified, the R3 test results are in line with value ranges for low-reactive materials, as reported for a broader set of SCMs, such as GGBFS, coal fly ash and calcined clay [31,33,44,45], which corresponds with the fairly modest strength activity results. Therefore, the R3 test seems to properly estimate the reactivity of NFM slags and can thus be recommended for further use for the same purpose. Sivakumar et al. [21] also concluded that the R3 test can be successfully used for the assessment of the reactivity of NFM slags. In contrast, TGA measurements for determining the portlandite consumption of the blended pastes were found to be similar for different slags and may not be easily related to slag reactivity, given the variation in the CaO content of the slags and the need for additional measurements or assumptions on hydration product stoichiometry. As such, due to their laboriousness and lack of contribution to the conclusions about the reactivity of the slags, portlandite consumption measurements are not recommended for future studies on such slags.

The reactivity of slag can be further improved by an increase in fineness [20] and more extensive modification of the chemical composition. From the presented results, an optimal region cannot be inferred for the chemical composition at this point. However, it appears that limiting the MgO and K_2O/SO_3 contents could have a positive effect on the strength development of slags. Literature data point to the potential benefits of further increasing CaO and Al_2O_3 levels [18]. Rapid water-jet cooling to maximise the amorphous content is also advisable for increasing the amorphous content and boosting reactivity [14]. Finally, modification of the reaction medium of slags would be of interest to increase their reactivity, for instance, by the addition of hydration accelerators such as Na_2SO_4 or $CaCl_2$ [46–48], optimisation of the sulphate content of the blended cement [49] and addition of fine limestone to enhance the early clinker hydration and maintain the ettringite levels high in the hydrated cements [50].

5. Conclusions

The findings of this research are summarised below:

- The application of a secondary thermal treatment to non-ferrous slags from the lead and copper industries can significantly reduce the amounts of heavy metals in the slags and enable their use in cementitious materials.

- Such slags are primarily composed of iron silicates. Despite the differences in the source and compositions of the slags, while granulation results in a substantial increase in their amorphous content, they are only moderately reactive according to R3 and calorimetry findings.
- Replacement of cement with such slags were found in all cases to result in an increase in the clinker degree of reaction in all ages, which is potentially due to the increase in the availability of water to cement grains.
- TGA results also indicate an acceleration in hydration reactions when cement is partially replaced by the studied slags. However, the portlandite and bound water contents of slag-blended mixtures in the early ages found to be lower than those of mixtures containing quartz powder. This is in agreement with the calorimetry results and indicates a slight retarding effect of such slags compared to quartz.
- While a notable increase in the porosity as well as coarsening of the pore size structure of cement paste mixtures was observed up to the age of 28 days as a result of cement substitution, a considerable refinement of the pore structure was detected at later ages. No such later-age refinement was observed for the pastes incorporating quartz powder.
- Despite the existence of sufficient evidence for the pozzolanic reactivity of the studied slags, the compressive strength of mortars prepared by such slags were found to be similar to that of mixtures containing quartz powder at different ages. This was attributed to the lower mechanical strength and filler effect of the slag grains compared to quartz powder.
- All three slags were found to satisfy the minimum strength activity and maximum leaching requirements and are thus suitable for use in concrete.
- While the slags were found to satisfy the minimum technical and environmental requirements for being used in concrete, it appears that mere granulation of such slags is not sufficient for promoting their pozzolanic activity. Addition of other oxides such as calcium or aluminium oxide to boost the reactivity is recommended.

Author Contributions: Conceptualisation, L.H., A.G.V. and R.S.; methodology, A.G.V., L.H., R.S., J.M. and B.F.; software, A.G.V. and P.T.; validation, L.H., R.S., A.P. and J.M.; formal analysis, A.G.V., P.T. and R.S.; investigation, A.G.V., L.H. and R.S.; resources, J.M., K.K., L.H. and R.S.; data curation, A.G.V., P.T., R.S. and J.M.; writing—original draft preparation, A.G.V., R.S., L.H. and A.P.; writing—review and editing, A.G.V., R.S., L.H., A.P., J.M. and K.K.; visualisation, A.G.V. and P.T.; supervision, R.S. and L.H.; project administration, L.H.; funding acquisition, L.H. and B.F. All authors have read and agreed to the published version of the manuscript.

Funding: This research was funded by the European Institute of Innovation and Technology (EIT) RawMaterials (grant number 17181).

Institutional Review Board Statement: Not applicable.

Informed Consent Statement: Not applicable.

Data Availability Statement: Not applicable.

Acknowledgments: The SlagVal project is a KIC Added Value Activity (KAVA) funded by the European Institute of Innovation and Technology (EIT) RawMaterials (Project No. 17181). The EIT is a body of the European Union and receives support from the European Union's Horizon 2020 Research and Innovation Programme.

Conflicts of Interest: The authors declare no conflict of interest. The funders had no role in the design of the study; in the collection, analyses or interpretation of data; in the writing of the manuscript; or in the decision to publish the results.

References

1. Bribián, I.Z.; Capilla, A.V.; Usón, A.A. Life cycle assessment of building materials: Comparative analysis of energy and environmental impacts and evaluation of the eco-efficiency improvement. *Build. Environ.* **2011**, *46*, 1113–1140.
2. Andrew, R.M. Global CO_2 emissions from cement production. *Earth Syst. Sci. Data* **2018**, *10*, 195–217. [CrossRef]

3. Ariño, A.M.; Mobasher, B. Effect of Ground Copper Slag on Strength and Toughness of Cementitious Mixes. *ACI Mater. J.* **1999**, *96*, 68–73.
4. Mindess, S.; Young, J.F.; Darwin, D. *Concrete*; Prentice Hall, Pearson Education, Inc.: Upper Saddle River, NJ, USA, 2003.
5. Boddy, A.M.; Hooton, R.D.; Thomas, M.D.A. The effect of product form of silica fume on its ability to control alkali-silica reaction. *Cem. Concr. Compos.* **2000**, *30*, 1139–1150. [CrossRef]
6. Atahan, H.N.; Dikme, D. Use of mineral admixtures for enhanced resistance against sulfate attack. *Constr. Build. Mater.* **2011**, *25*, 3450–3457. [CrossRef]
7. Pan, D.A.; Li, L.; Tian, X.; Wu, Y.; Cheng, N.; Yu, H. A review on lead slag generation, characteristics, and utilization. *Resour. Conserv. Recycl.* **2019**, *146*, 140–155. [CrossRef]
8. Gorai, B.; Jana, R.K. Characteristics and utilisation of copper slag—A review. *Resour. Conserv. Recy.* **2003**, *39*, 299–313. [CrossRef]
9. Curry, K.C. *Iron and Steel Slag*; U.S. Geological Survey, Mineral Commodity Summaries: Reston, VA, USA, 2020.
10. Piatak, N.M.; Parsons, M.B.; Seal, R.R. Characteristics and environmental aspects of slag: A review. *Appl. Geochem.* **2015**, *57*, 236–266. [CrossRef]
11. Li, W.; Tang, Z.; Tam, V.; Zhao, X.; Wang, K.F. A Review on Durability of Alkali-activated System from Sustainable Construction Materials to Infrastructures. *Es Mater. Manuf.* **2019**, *4*, 2–19. [CrossRef]
12. Barati, M.; Jahanshahi, S. Granulation and Heat Recovery from Metallurgical Slags. *J. Sustain. Metall.* **2019**, *6*, 191–206. [CrossRef]
13. De Rojas, M.I.S.; Rivera, J.; Frias, M.; Marin, F. Use of recycled copper slag for blended cements. *J. Chem. Technol. Biot.* **2008**, *83*, 209–217. [CrossRef]
14. Pontikes, Y.; Machiels, L.; Onisei, S.; Pandelaers, L.; Geysen, D.; Jones, P.T.; Blanpain, B. Slags with a high Al and Fe content as precursors for inorganic polymers. *Appl. Clay Sci.* **2013**, *73*, 93–102. [CrossRef]
15. Siakati, C.; Douvalis, A.P.; Ziogas, P.; Peys, A.; Pontikes, Y. Impact of the solidification path of FeOx-SiO2 slags on the resultant inorganic polymers. *J. Am. Ceram Soc.* **2019**, *103*, 2173–2184. [CrossRef]
16. Feng, Y.; Yang, Q.; Chen, Q.; Kero, J.; Andersson, A.; Ahmed, H.; Engström, F.; Samuelsson, C. Characterization and evaluation of the pozzolanic activity of granulated copper slag modified with CaO. *J. Clean. Prod.* **2019**, *232*, 1112–1120. [CrossRef]
17. Sivakumar, P.P.; Arnout, L.; Lapauw, T.; Gruyaert, E.; De Belie, N.L.; Matthys, S. Increasing the Reactivity of Modified Ferro Silicate Slag by Chemical Adaptation of the Production Process. In Proceedings of the 2nd International Conference on Sustainable Building Materials, Eindhoven, The Netherlands, 12–15 August 2019; pp. 36–46.
18. Van De Sande, J.; Peys, A.; Hertel, T.; Rahier, H.; Pontikes, Y. Upcycling of non-ferrous metallurgy slags: Identifying the most reactive slag for inorganic polymer construction materials. *Resour. Conserv. Recycl.* **2020**, *154*, 104627. [CrossRef]
19. Edwin, R.S.; De Schepper, M.; Gruyaert, E.; De Belie, N. Effect of secondary copper slag as cementitious material in ultra-high performance mortar. *Constr Build Mater* **2016**, *119*, 31–44. [CrossRef]
20. Hallet, V.; De Belie, N.; Pontikes, Y. The impact of slag fineness on the reactivity of blended cements with high-volume non-ferrous metallurgy slag. *Constr. Build. Mater.* **2020**, *257*, 119400. [CrossRef]
21. Sivakumar, P.P.; Matthys, S.; De Belie, N.; Gruyaert, E. Reactivity Assessment of Modified Ferro Silicate Slag by R3 Method. *Appl. Sci.* **2021**, *11*, 366. [CrossRef]
22. Kriskova, L.; Pontikes, Y.; Pandelaers, L.; Cizer, Ö.; Jones, P.T.; Van Balen, K.; Blanpain, B. Effect of High Cooling Rates on the Mineralogy and Hydraulic Properties of Stainless Steel Slags. *Metall. Mater. Trans. B* **2013**, *44*, 1173–1184. [CrossRef]
23. Matthes, W.; Vollpracht, A.; Villagrán, Y.; Kamali-Bernard, S.; Hooton, D.; Gruyaert, E.; Soutsos, M.; De Belie, N. Ground granulated blast-furnace slag. In *Properties of Fresh and Hardened Concrete Containing Supplementary Cementitious Materials*; Springer: Berlin/Heidelberg, Germany, 2018; pp. 1–53.
24. Vollpracht, A.; Brameshuber, W. Binding and leaching of trace elements in Portland cement pastes. *Cem. Concr. Res.* **2016**, *79*, 76–92. [CrossRef]
25. Van der Sloot, H.A. Comparison of the characteristic leaching behavior of cements using standard (EN 196-1) cement mortar and an assessment of their long-term environmental behavior in construction products during service life and recycling. *Cem. Concr. Res.* **2000**, *30*, 1079–1096. [CrossRef]
26. Saikia, N.; Cornelis, G.; Mertens, G.; Elsen, J.; Van Balen, K.; Van Gerven, T.; Vandecasteele, C. Assessment of Pb-slag, MSWI bottom ash and boiler and fly ash for using as a fine aggregate in cement mortar. *J. Hazard. Mater.* **2008**, *154*, 766–777. [CrossRef]
27. Skibsted, J.; Snellings, R. Reactivity of supplementary cementitious materials (SCMs) in cement blends. *Cem. Concr. Res.* **2019**, *124*, 105799. [CrossRef]
28. Gholizadeh Vayghan, A.; Wright, J.R.; Rajabipour, F. An extended chemical index model to predict the fly ash dosage necessary for mitigating alkali–silica reaction in concrete. *Cem. Concr. Res.* **2016**, *82*, 1–10. [CrossRef]
29. EN. *BS EN 197-1. Cement. Composition, Specifications and Conformity Criteria for Common Cements*; BSI: Brussels, Belgium, 2011.
30. Avet, F.; Scrivener, K. Effect of temperature on the water content of CASH in plain Portland and blended cements. *Cem. Concr. Res.* **2020**, *136*, 106124. [CrossRef]
31. Avet, F.; Snellings, R.; Alujas Diaz, A.; Ben Haha, M.; Scrivener, K. Development of a new rapid, relevant and reliable (R3) test method to evaluate the pozzolanic reactivity of calcined kaolinitic clays. *Cem. Concr. Res.* **2016**, *85*, 1–11. [CrossRef]
32. Snellings, R.; Scrivener, K.L. Rapid screening tests for supplementary cementitious materials: Past and future. *Mater. Struct.* **2016**, *49*, 3265–3279. [CrossRef]

33. Li, X.; Snellings, R.; Antoni, M.; Alderete, N.M.; Haha, M.B.; Bishnoi, S.; Cizer, Ö.; Cyr, M.; De Weerdt, K.; Dhandapani, Y. Reactivity tests for supplementary cementitious materials: RILEM TC 267-TRM phase 1. *Mater. Struct.* **2018**, *51*, 1–14. [CrossRef]
34. Snellings, R. X-ray powder diffraction applied to cement. In *A Practical Guide to Microstructural Analysis of Cementitious Materials*; Scrivener, K.L., Snellings, R., Lothenbach, B., Eds.; CRC Press: Boca Raton, FL, USA, 2016; pp. 107–176.
35. Ronneberger, O.; Fischer, P.; Brox, T. Convolutional Networks for Biomedical Image Segmentation. In Proceedings of the 18th International Conference on Medical Image Computing and Computer-Assisted Intervention, Munich, Germany, 5–9 October 2015; pp. 234–241.
36. EN. *BS EN 196-1: Methods of Testing Cement—Part 1: Determination of Strength*; BSI: Brussels, Belgium, 2005.
37. EN. *BS EN 1015-3. Methods of Test for Mortar for Masonry. Determination of Consistence of Fresh Mortar (by Flow Table)*; BSI: Brussels, Belgium, 1999.
38. EN. *BS EN 12457-4. Characterisation of Waste. Leaching. Compliance Test for Leaching of Granular Waste Materials and Sludges. One Stage Batch Test at a Liquid to Solid Ratio of 10 l/kg for Materials with Particle Size below 10 mm (without or with Size Reduction)*; BSI: Brussels, Belgium, 2002.
39. EN. *EN 15167-1: Ground Granulated Blast Furnace Slag for Use in Concrete, Mortar and Grout—Part 1: Definitionhs, Specifications and Conformity Criteria*; BSI: Brussels, Belgium, 2006.
40. Weeks, C.; Hand, R.J.; Sharp, J.H. Retardation of cement hydration caused by heavy metals present in ISF slag used as aggregate. *Cem. Concr. Compos.* **2008**, *30*, 970–978. [CrossRef]
41. Asavapisit, S.; Fowler, G.; Cheeseman, C.R. Solution chemistry during cement hydration in the presence of metal hydroxide wastes. *Cem. Concr. Res.* **1997**, *27*, 1249–1260. [CrossRef]
42. Cheeseman, C.R.; Asavapisit, S. Effect of calcium chloride on the hydration and leaching of lead-retarded cement. *Cem. Concr. Res.* **1999**, *29*, 885–892. [CrossRef]
43. Spooren, J.; Binnemans, K.; Björkmalm, J.; Breemersch, K.; Dams, Y.; Folens, K.; González-Moya, M.; Horckmans, L.; Komnitsas, K.; Kurylak, W. Near-zero-waste processing of low-grade, complex primary ores and secondary raw materials in Europe: Technology development trends. *Resour. Conserv. Recycl.* **2020**, *160*, 104919. [CrossRef]
44. Blotevogel, S.; Ehrenberg, A.; Steger, L.; Doussang, L.; Kaknics, J.; Patapy, C.; Cyr, M. Ability of the R3 test to evaluate differences in early age reactivity of 16 industrial ground granulated blast furnace slags (GGBS). *Cem. Concr. Res.* **2020**, *130*, 105998. [CrossRef]
45. Snellings, R.; Kamyab, H.; Joseph, S.; Nielsen, P.; Loots, M.; Abeele, L.V.d. Pozzolanic Reactivity of Size-Classified Siliceous Fly Ashes. In Proceedings of the 2nd International Conference of Sustainable Building Materials, Eindhoven, The Netherlands, 12–15 August 2019.
46. Shi, C.; Day, R.L. Comparison of different methods for enhancing reactivity of pozzolans. *Cem. Concr. Res.* **2001**, *31*, 813–818. [CrossRef]
47. Rashad, A.; Bai, Y.; Basheer, P.; Milestone, N.; Collier, N. Hydration and properties of sodium sulfate activated slag. *Cem. Concr. Compos.* **2013**, *37*, 20–29. [CrossRef]
48. Joseph, S.; Snellings, R.; Cizer, Ö. Activation of Portland cement blended with high volume of fly ash using Na_2SO_4. *Cem. Concr. Compos.* **2019**, *104*, 103417. [CrossRef]
49. Adu-Amankwah, S.; Black, L.; Skocek, J.; Haha, M.B.; Zajac, M. Effect of sulfate additions on hydration and performance of ternary slag-limestone composite cements. *Constr. Build. Mater.* **2018**, *164*, 451–462. [CrossRef]
50. Adu-Amankwah, S.; Lopez, S.A.B.; Black, L. Influence of component fineness on hydration and strength development in ternary slag-limestone cements. *Rilem Tech. Lett.* **2019**, *4*, 81–88. [CrossRef]